

# Dislocation Annealing in Fine-Grained Synthetic Olivine

R. J. M. Farla, H. Kokkonen, J. D. Fitz Gerald and I. Jackson

*Research School of Earth Sciences, Australian National University, Canberra, ACT 0200, Australia.*

Multiple specimens from a pre-deformed synthetic olivine polycrystal were subjected to static annealing for periods of ~3-50h at temperatures of 1100-1450°C under a controlled furnace atmosphere. Changes in dislocation density obey a second-order rate equation describing dislocation recovery with an activation energy of  $308 \pm 26 \text{ kJ mol}^{-1}$ . Micro-structural analysis reveals substantial dislocation re-organisation within grains and sub-grain formation.

## 1. Introduction

The evolution of dislocation structures in  $(\text{Mg}_{0.9}\text{Fe}_{0.1})_2\text{SiO}_4$  olivine, from formation in the dislocation creep field to static and dynamic recovery, is important to the rheological understanding of the Earth's upper mantle. In addition, establishing the rates of change for dislocation density in synthetic olivine provides new opportunities for determining the effect of dislocation density on damping of seismic waves.

Dislocations are line defects in the crystal lattice where otherwise perfect atomic arrangements are disrupted. At low temperature under high stress, dislocations are impeded by obstacles as they glide in their slip plane and pile ups generate back-stresses on sources that oppose further emission. Strain cannot continue until some leading dislocations pass/jump the obstacle. This is called work hardening. At high temperatures ( $>1000^\circ\text{C}$ ), however, dislocation climb and cross-slip takes over. Now dislocations have an extra degree of freedom for movement which leads to a reduction in the dislocation density and dislocations untangle. This is called recovery or dislocation annealing. The dislocation density is measured by the total dislocation line length per unit volume (or the number of dislocations per unit area) and the recovery thereof is a function of temperature, pressure, time and oxygen fugacity.

The results of this study offer a solid prediction of the evolution of dislocation density for synthetic olivine as a function of temperature and annealing time. In addition, the activation energy of dislocation recovery is determined and some constraints on the dislocation recovery mechanisms are evaluated.

## 2. Sample preparation

Synthetic dry iron-bearing olivine has been prepared via the solgel method [1]. A dense polycrystalline aggregate was prepared by hot pressing. It was subsequently deformed with increasing loads producing a final strain step of 2% strain under 253 MPa of uniaxial compressive stress. Total strain was about 19% at 1250°C and 300 MPa argon gas confining pressure. The recovered specimen was cut up and the resulting samples were used for the annealing experiments.

The annealing experiments are summarized in Table 1. The experiments (for temperatures ranging from 1100-1450°C and annealing times 3.5-50.5 h) were performed in a furnace capable of achieving temperatures up to 1600°C under controlled oxygen fugacity conditions at 1 bar within the olivine stability field.

A gas mix of 70% CO and 30% CO<sub>2</sub> was used. The olivine specimens were placed in a platinum cup fitted with thin platinum wires on the bottom to ensure minimal contact with the

metal. The temperature was ramped up at 12°C/min for each experiment. After annealing, the temperature was ramped down by switching off the furnace to prevent any further dislocation annealing during cooling. The samples were not quenched in water, however, to avoid major cracking.

After annealing, the sample surface was ground back by approximately 80 micron (SiC 600, 1200) and then highly polished. An oxidation–decoration technique was used to reveal the dislocations [2]. The oxidised sample surface was then further polished with alumina slurry (0.05 micron) for 10 minutes to expose the dislocations. An Hitachi 4300SE FESEM was used to image the decorated dislocations at a magnification of x8000 and an accelerating voltage of 5kV. This was performed by taking images in a grid pattern. The total area  $A$  across all images is about 5,000  $\mu\text{m}^2$  or more. Using image manipulation software (ImageJ) the final dislocation density,  $\rho_f$  was estimated as  $\Sigma \{l_a \sqrt{1+(l_d/l_a)^2}/Al_d\}$  involving correction of the projected length  $l_a$  for the effect of the electron penetration depth,  $l_d$  ( $l_d \sim 0.3\mu\text{m}$  at 5kV accelerating voltage). The uncertainty was obtained by dividing the total area per sample into small areas of about 300  $\mu\text{m}^2$ . The dislocation density was then calculated as the mean of those for all  $\sim 300 \mu\text{m}^2$  areas with an uncertainty given by the standard error in the mean. The initial dislocation density, similarly measured, was  $\rho_i = 4.09 \pm 0.41 \mu\text{m}^{-2}$ .

Table 1. Summary of all annealing experiments (and original material). The \* indicates an experiment in which the gas mix was adjusted to obtain the same  $f_{\text{O}_2}$  as at 1300°C for a CO/CO<sub>2</sub> 70/30 mix.

Sample	T (°C)	$f_{\text{O}_2}$ (10 <sup>-6</sup> Pa)	$t$ (h)	$\rho_i$ (10 <sup>12</sup> m <sup>-2</sup> )	$\rho_f$ (10 <sup>12</sup> m <sup>-2</sup> )	<i>Disl anneal rate</i> $k$ (10 <sup>-14</sup> m <sup>2</sup> s <sup>-1</sup> )	Recovery (%)	Grain size, $d$ (10 <sup>6</sup> m)	Porosity (%)
Fo-01	1450	75	3.5	4.09±0.41	1.48±0.20	34.2±7.50	63±6	4.61±0.21	14.3
Fo-02	1400	23	3.5	4.09±0.41	2.10±0.25	18.4±4.57	49±8	3.85±0.17	3.8
Fo-03	1350	6.4	3.5	4.09±0.41	2.75±0.31	9.46±3.27	33±9	3.77±0.23	3.0
Fo-04	1300	1.7	3.5	4.09±0.41	3.20±0.37	5.40±2.49	21±9	3.79±0.19	1.9
Fo-05	1300	1.7	8.5	4.09±0.41	2.56±0.30	4.78±1.28	37±8	3.94±0.25	2.0
Fo-06	1300	1.7	16.5	4.09±0.41	2.25±0.20	3.37±1.08	45±9	3.82±0.21	2.8
Fo-07	1300	1.7	50.5	4.09±0.41	1.30±0.23	2.92±1.06	68±8	3.77±0.23	3.1
Fo-08	1200	0.086	50.5	4.09±0.41	2.00±0.20	1.42±0.45	49±8	3.44±0.19	1.9
Fo-08*	1200	1.7	50.5	4.09±0.41	2.07±0.20	1.33±0.35	51±9	3.54±0.20	2.0
Fo-09	1100	0.0029	50.5	4.09±0.41	3.58±0.25	0.19±0.21	12±13	3.63±0.19	1.7
Fo-00	-	-	-	4.09±0.41	-	-	-	3.72±0.15	1.9

### 3. Results and discussion

Fig. 1 contrasts the dislocation microstructure between the as-deformed and annealed olivines. Notice the significant decrease in dislocation density and sub-grain formation (see arrows) in the annealed sample. The dislocation loss seems to have affected curved dislocations the most. The circled area is an example of a grain in which the dislocations have aligned themselves in a particular direction, presumably on one of the major slip planes in olivine. It would appear these are relatively stable configurations for dislocations as, after annealing at higher temperatures, samples exhibit the same features. It is not known whether much more annealing is possible. It is unlikely that all dislocations will be recovered on laboratory time scales.

The annealing data fit the following empirical second-order recovery equation:

$$\frac{d\rho}{dt} = -\rho^2 k \quad (1)$$

$$k = k_0 \exp\left(-\frac{E_a + PV^*}{RT}\right) \quad (2)$$

where  $\rho$  is the dislocation density,  $E_a$  is the activation energy for dislocation recovery,  $P$  is pressure,  $V^*$  is the activation volume,  $R$  is the gas constant,  $T$  is temperature and  $k_0$  is a constant. Eq. (1) can be integrated to give the following expression

$$1/\rho_f - 1/\rho_i = kt \quad (3)$$

against which the data in Table 1 are plotted in Fig. 2. That dislocation recovery appears to be a second-order process may reflect annihilation resulting from dislocation interaction as opposed to simple dislocation glide out into the grain boundaries.

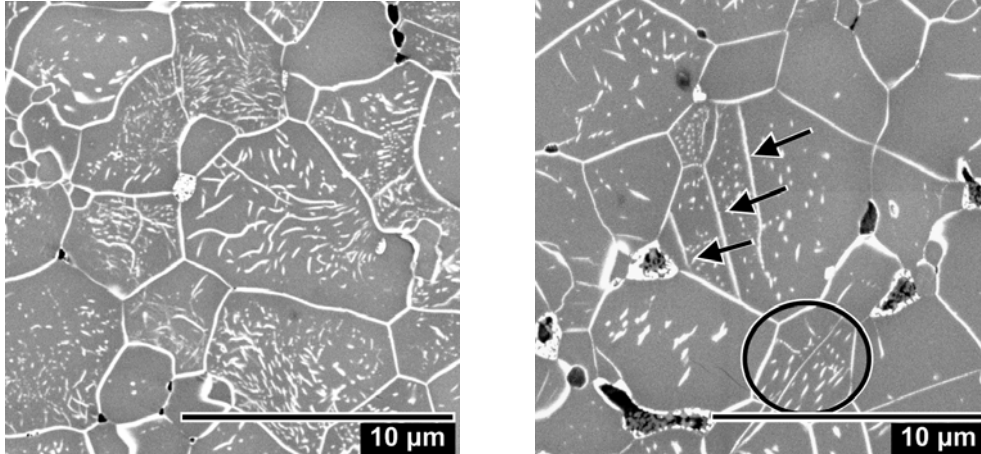


Fig 1. FESEM electron micrographs of synthetic deformed olivine (left) and the same material (right) annealed at 1300°C for 50.5 hours.

$E_a$  is found to be  $308 \pm 26 \text{ kJ mol}^{-1}$ , whereas for natural polycrystalline olivine the activation energy is found to be  $398 \pm 59 \text{ kJ mol}^{-1}$  [4]. The overall dislocation recovery rate is lower by one [5] to two orders of magnitude [3,4]. For studies [3] and [5] natural single crystal olivine was used and the activation energy for [3] is  $323 \pm 18 \text{ kJ mol}^{-1}$ . Dislocation recovery in synthetic olivine is thus markedly slower than that in natural olivine without a significantly different activation energy. As shown in Fig. 2 on the right, the empirical relationship predicts well the percentage of dislocation recovery with time and temperature.

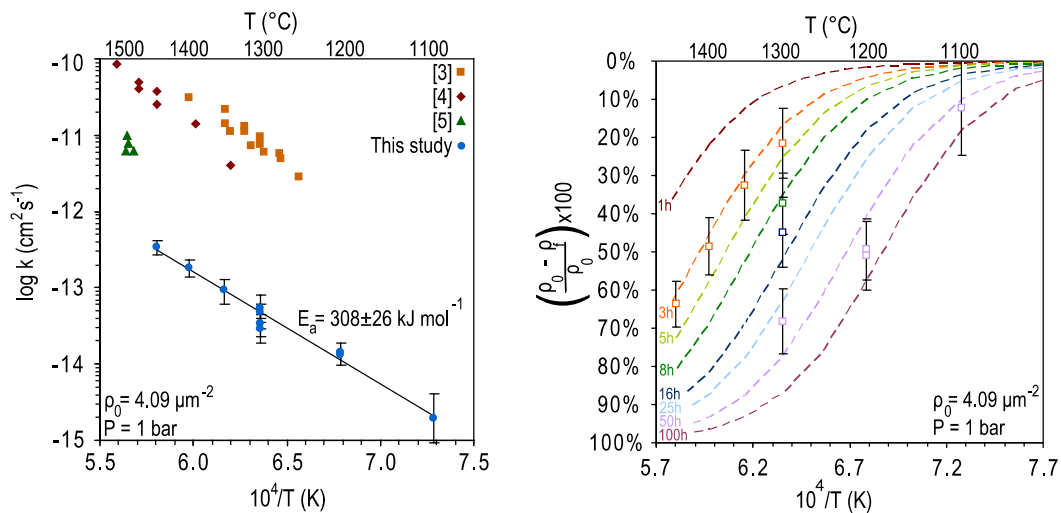


Fig 2. Left: dislocation recovery rate versus reciprocal of temperature (1450°C to 1100°C). Right: percent annealing versus reciprocal temperature. The annealing time curves are labelled accordingly. Errors have been calculated via error propagation.

The difference between current data and previous data can be attributed to several factors. First of all it is unwise to compare single crystal data with polycrystalline data

because, in the latter, multiple slip systems are activated and in the former only one. Also the significant impurity content of natural olivine (e.g. substitutional atoms like Al and Cr) may result in different behaviour than in synthetic olivine. This would also apply to the presence of other phases, such as spinel, in natural material. There are also differences in grain size and hence dislocation length. With grain boundaries being a source and sink for vacancies one would, in fact, expect materials with a small grain size to undergo faster dislocation annealing which is not observed. Furthermore, the silica activity was previously not controlled whereas in this study olivine was stabilised with the addition of orthopyroxene which buffers the silica activity. This results in a controlled Si vacancy concentration. Current experiments were performed with a gas mix 70/30 CO/CO<sub>2</sub> to approximate the temperature dependent  $f_{O_2}$  from thermodynamic calculations for an Ol-Fe/Ni buffer. There may be an effect of oxygen fugacity on dislocation annealing [8] although this is not very pronounced as seen by the two data points in Fig. 2 at 1200°C and 50.5 hours of annealing. Lastly, for one study [4] the optical microscope was used to image dislocations whereas in this study and the one from 1993, [5] the SEM was used. In the third study on single crystal olivine [3] the TEM was used with the drawback of only sampling small areas (~24 micrographs at 54  $\mu\text{m}^2$ ). The SEM allows for a much higher resolution for relatively large areas. In this study, dislocations as close as 100nm were effectively distinguished from one another for areas between 5000 and 9000  $\mu\text{m}^2$ .

#### 4. Conclusions

There is a systematic dislocation recovery dependence for synthetic polycrystalline olivine on time and temperature, the two major variables. The activation energy,  $E_a = 308 \pm 26 \text{ kJ mol}^{-1}$  for static dislocation recovery under atmospheric pressure compares quite well with previous results although the dislocation annealing rate is markedly lower. These experiments will serve as a prediction tool for planned seismic attenuation experiments on similar synthetic deformed material. Seismic attenuation runs typically last a week starting at the highest practicable temperature followed by staged cooling. It is not uncommon to wait ~50 hours at the starting temperature before the microstructure in the olivine specimen has stabilised. Thus to avoid significant dislocation recovery on timescales of ~50 hours a maximum temperature of  $\leq 1100^\circ\text{C}$  is required.

#### Acknowledgments

We thank Ulrich Faul and Auke Barnhoorn for useful discussions and assistance for calculating the uncertainty in the data. This research is supported by an International Endeavour Post-graduate Research scholarship (IEPRS).

#### References

- [1] R. D. McDonnell, C. J. Spiers and C. J. Peach, *Phys. Chem. Min.* **29**, 19 (2002).
- [2] D. L. Kohlstedt, C. Goetze, W. B. Durham, and J. Vandersande, *Science*. **191**, 1045 (1976)
- [3] D. L. Kohlstedt, H. P. K. Nichols and P. Hornack, *J. Geophys. Res.* **85**, 3122 (1980)
- [4] S. Karato and M. Ogawa, *Phys. Earth Planet. Inter.* **28**, 102 (1982)
- [5] S. Karato, D. C. Rubie and H. Yan, *J. Geophys. Res.* **98**, 9761 (1993)
- [6] O. Jaoul, *J. Geophys. Res.* **95**, 17631 (1990)
- [7] J. Weertman, *Rev. Geophys. Space Phys.* **8**, 145 (1970)
- [8] S. Karato and H. Sato, *Phys. Earth Planet. Inter.* **28**, 312 (1982)